Geobiology

Geobiology (2011), 9, 61–78 DOI: 10.1111/j.1472-4669.2010.00257.x

The methane cycle in ferruginous Lake Matano

S. A. CROWE,[1,2,3] S. KATSEV,[1,4] K. LESLIE,[2] A. STURM,[2] C. MAGEN,[1,3] S. NOMOSATRYO,[5] M. A. PACK,[6] J. D. KESSLER,[7] W. S. REEBURGH,[6] J. A. ROBERTS,[2] L. GONZÁLEZ,[2] G. DOUGLAS HAFFNER,[8] A. MUCCI,[1,3] B. SUNDBY[1,9] AND D. A. FOWLE[2]

[1]*Earth and Planetary Sciences, McGill University, Montréal, Québec, Canada*
[2]*Department of Geology, University of Kansas, Lawrence, Kansas, USA*
[3]*GEOTOP, Université du Québec à Montréal, Montréal, Québec, Canada*
[4]*Large Lakes Observatory (LLO), University of Minnesota, Duluth, Minnesota, USA*
[5]*Research Center for Limnology, Indonesian Institute of Sciences (LIPI), Cibinong-Bogor, Indonesia*
[6]*Department of Earth System Science, University of California Irvine, Irvine, California, USA*
[7]*Department of Oceanography, Texas A & M University, College Station, Texas, USA*
[8]*Great Lakes Institute for Environmental Research (GLIER), University of Windsor, Windsor, Ontario, Canada*
[9]*ISMER, Université du Québec à Rimouski, Rimouski, Québec, Canada*

ABSTRACT

In Lake Matano, Indonesia, the world's largest known ferruginous basin, more than 50% of authigenic organic matter is degraded through methanogenesis, despite high abundances of Fe (hydr)oxides in the lake sediments. Biogenic CH_4 accumulates to high concentrations (up to 1.4 mmol L^{-1}) in the anoxic bottom waters, which contain a total of 7.4×10^5 tons of CH_4. Profiles of dissolved inorganic carbon (ΣCO_2) and carbon isotopes ($\delta^{13}C$) show that CH_4 is oxidized in the vicinity of the persistent pycnocline and that some of this CH_4 is likely oxidized anaerobically. The dearth of NO_3^- and SO_4^{2-} in Lake Matano waters suggests that anaerobic methane oxidation may be coupled to the reduction of Fe (and/or Mn) (hydr)oxides. Thermodynamic considerations reveal that CH_4 oxidation coupled to Fe(III) or Mn(III/IV) reduction would yield sufficient free energy to support microbial growth at the substrate levels present in Lake Matano. Flux calculations imply that Fe and Mn must be recycled several times directly within the water column to balance the upward flux of CH_4. 16S gene cloning identified methanogens in the anoxic water column, and these methanogens belong to groups capable of both acetoclastic and hydrogenotrophic methanogenesis. We find that methane is important in C cycling, even in this very Fe-rich environment. Such Fe-rich environments are rare on Earth today, but they are analogous to conditions in the ferruginous oceans thought to prevail during much of the Archean Eon. By analogy, methanogens and methanotrophs could have formed an important part of the Archean Ocean ecosystem.

Received 21 February 2010; accepted 4 August 2010

Corresponding authors: Sean A. Crowe. Tel.: +45 6550 2795; fax: +45 6593 0457; e-mail: sacrowe1@gmail.com;
David A. Fowle. Tel.: +1 785 864 1955; fax: +1 785 864 5276; e-mail: fowle@ku.edu

INTRODUCTION

Nearly 600 m deep, Lake Matano in Indonesia is one of the deepest lakes on Earth, and its anoxic waters comprise the world's largest known Fe(II)-rich (ferruginous) basin (Crowe *et al.*, 2008a,b). Lateritic soils consisting of up to 60 wt.% Fe (hydr)oxides dominate the surficial geology of Lake Matano's catchment basin (Golightly, 1981; Crowe *et al.*, 2008b) and erosion of these soils supplies Fe-rich particulate matter to Lake Matano. The water column of Lake Matano exhibits weak thermal gradients, yet a persistent pycnocline is located at around 100 m depth, forming a boundary between the well-mixed, oxic surface water and the anoxic bottom water (Crowe *et al.*, 2008b; Katsev *et al.*, 2010). Exchange of water across this pycnocline is slow and occurs on a millennial time scale, similar to temperate meromictic lakes (Crowe *et al.*, 2008b; Katsev *et al.*, 2010). Owing to this slow exchange and the very low concentrations of dissolved S (i.e., SO_4^{2-} and $\Sigma S(-II)$), ferrous Fe has accumulated to high concentrations in the anoxic bottom waters (Crowe *et al.*, 2008b). Slow exchange of water also favors the accumulation of dissolved gases. Indeed, dissolved

gases (CH_4 and CO_2) are known to accumulate to high concentrations in a number of the world's permanently stratified lakes, including Lake Kivu in East Africa (Schmid *et al.*, 2005) and Lake Pavin in France (Lehours *et al.*, 2009). Our study of the biogeochemical cycling of CH_4 (and CO_2) in Lake Matano was initially prompted by concern that these gases might reach levels that could cause a limnic eruption, similar to the catastrophic events in Lakes Nyos and Lagos in Africa (Zhang & Kling, 2006).

Additional motivation for this study arose from Lake Matano's status as an end member sulfur-poor, iron-rich environment. These chemical conditions and the stratified nature of Lake Matano support a novel and unique microbial ecology, including recently discovered low-light adapted Chlorobiaceae (Crowe *et al.*, 2008a). The ubiquity of SO_4^{2-} in most modern environments intrinsically links the CH_4 and S cycles because the rates and pathways of both methanogenesis and methanotrophy are directly influenced by SO_4^{2-} availability (Capone & Kiene, 1988; Reeburgh, 2007). The scarcity of dissolved SO_4^{2-} in Lake Matano may foster an atypical CH_4 cycle, likely precluding SO_4^{2-}-based anaerobic CH_4 oxidation and favoring aerobic CH_4 oxidation or anaerobic CH_4 oxidation via alternative electron acceptors (Zehnder & Brock, 1980; Konhauser *et al.*, 2005; Caldwell *et al.*, 2008; Beal *et al.*, 2009). In this study, we used geochemical and microbiological techniques to elucidate the pathways of methane production and consumption, characterize Archaeal ecology, quantify the importance of CH_4 to carbon cycling in a SO_4^{2-}-poor environment, and evaluate the potential risk of methane-driven limnic eruption in Lake Matano. We also discuss the potential for CH_4 cycling in other ferruginous environments, including the Archean Ocean.

METHODS

Sampling and sample storage

Sampling was conducted at a central, deep-water location (2°28′00″S and 121°17′00″E) (Fig. 1) in July 2006 (end of the wet season) and February 2007 (beginning of the wet season) using local fishing boats. All water samples were collected with 5 L Go-Flow (Niskin; General Oceanics, Miami, FL, USA) bottles attached in series to a stainless steel cable and a hand-operated winch. The bottles were placed at depth to an accuracy of ±1 m with the help of a commercial fish finder (Furuno, FCV 585; Furuno Electric Co., Nishinomiya, Japan). Water samples for methane determination were drawn directly from the spigot of the Niskin bottle using a 60 mL syringe and immediately transferred from the syringe to pre-evacuated 14-mL crimp-sealed serum vials that had been flushed with N_2 gas and contained 100 μL of a saturated $HgCl_2$ solution to prevent further microbial methane production or oxidation. The partially filled serum vials were stored upside down to prevent potential leakage of CH_4 around the stopper. Total alkalinity was determined on water samples transferred to glass bottles and preserved with $HgCl_2$. Samples for the determination of total dissolved inorganic carbon (ΣCO_2) and NH_4^+ were drawn from the spigots with a 1 mL syringe and injected directly into a flow-injection analysis system (see below).

Analyses

Water temperature and conductivity profiles were collected *in situ* using a submersible Conductivity-Temperature-Depth probe (CTD) (Sea-Bird, SBE-19; Sea-Bird Electronics,

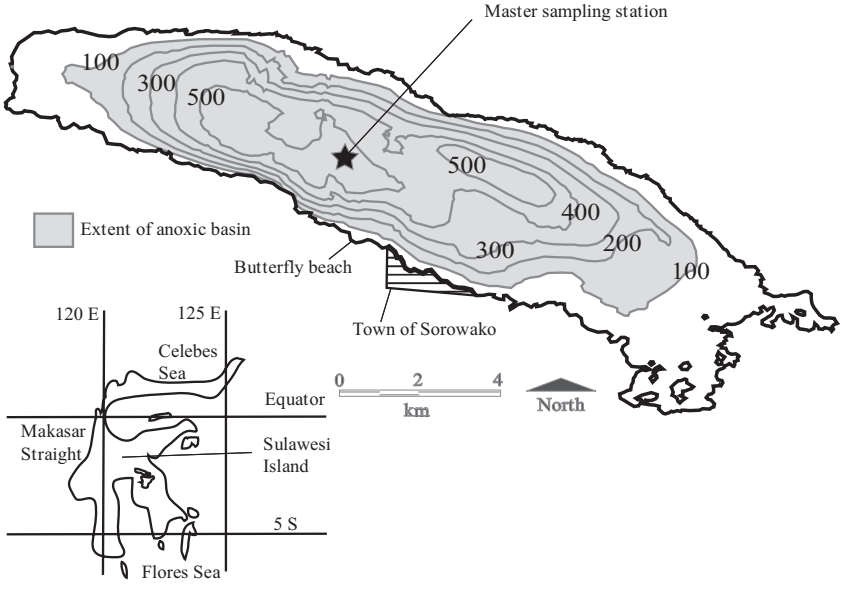

Fig. 1 Bathymetric map showing the locations of our deep water, master sampling station, the town of Sorowako, Butterfly beach, and the extent of the anoxic basin (modified after Crowe *et al.*, 2008b).

Bellevue, WA, USA). Methane concentrations in the headspace of the crimp-sealed vials were determined by gas chromatography (Agilent 6890N; Agilent Technologies, Santa Clara, CA, USA, with a HayeSep Q 80/100 column) with flame ionization (detection limit of 10^{-7} mmol L^{-1} and a precision of <1%, 2006) or thermal conductivity (detection limit of 2×10^{-5} mmol L^{-1} and a precision of <1%, 2007) detection. Total alkalinity was determined by potentiometric titration with a dilute HCl solution (Gieskes & Rogers, 1973) using an automated Radiometer titrator (Titrilab 865; Radiometer Analytical SAS, Lyon, France) with a reproducibility of better than 0.5%. The ΣCO_2 and dissolved NH_4^+ concentrations were measured by flow injection analysis (Hall & Aller, 1992). Detection limits were <50 μmol L^{-1} and 0.5 μmol L^{-1} for ΣCO_2 and NH_4^+, respectively, with a relative precision of better than 5%. The isotopic composition ($\delta^{13}C$) of CH_4 and CO_2 in headspace samples was determined by gas chromatography-combustion-isotope ratio mass spectrometry (GC-C-IRMS) using a ThermoFinnigan MAT 253 (Thermo Fisher Scientific, Waltham, MA, USA) mass spectrometer interfaced to a ThermoElemental Trace GC Ultra with a Rt-QPLOT column (Restek; Restek Corporation, Bellefonte, PA, USA). $\delta^{13}C_{\Sigma CO2}$ was determined by converting ΣCO_2 to gaseous CO_2 following the addition of concentrated orthophosphoric acid to the samples under a 15-mTorr vacuum. Water vapor was eliminated by double trapping, first with a liquid N_2-trap and followed by a dry-ice isopropyl alcohol trap. $\delta^{13}C$ measurements were made using a VG-Prism™ triple-collector mass spectrometer (Isoprime, Cheadle Hulme, UK). All stable C isotopic compositions are reported in per mil (‰) relative to the V-PDB standard with a precision of better than 0.2‰. Duplicate measurements of $\delta^{13}C_{\Sigma CO2}$ in water recovered from 110 m depth yielded values of −8.70‰ and −8.85‰ and were within the reported uncertainty. Samples of particulate organic matter (POM) were collected on pre-combusted 0.45 μm glass fiber filters. Portions of these filters were analyzed for nitrogen and carbon using an elemental analyzer.

Dissolved oxygen (DO) measurements were made by linear sweep voltammetry using an Analytical Instrument Systems (AIS) (Flemington, NJ, USA) DLK-60 with cell stand. Water samples were transferred directly from the Niskin bottles to a glass voltammetric cell via Tygon tubing. The cell was sealed from the atmosphere using rubber stoppers and o-rings and was flushed with three times the cell volume of water before measurement. Measurements were conducted with a three-electrode configuration using a Au–Hg amalgam microelectrode (50 μm radius), a saturated Ag–AgCl electrode, and a platinum wire as the working, reference, and counter electrodes, respectively (Luther *et al.*, 2003). The DO detection limit was 2.5 μmol L^{-1} based on three times the standard deviation of five measurements conducted in lake water purged for 15 min with N_2 gas that had been scrubbed through a catechol solution to remove traces of O_2 from the commercial, compressed N_2. Fe, Mn, and S species were determined as previously described (Crowe *et al.*, 2008a,b). NO_3^- and NO_2^- concentrations were determined spectrophotometrically using a 5-m long cell path (Yao *et al.*, 1998). Unfortunately, high reagent blanks precluded us from reaching the single-digit nmol L^{-1} detection limits previously attained (Yao *et al.*, 1998).

Samples used to measure the natural radiocarbon content of CH_4 were collected in 15-mL serum vials with an average nitrogen headspace of 5.5 mL from depths of 105, 112, 118, 130, 140, 160, 200, 250, 350, 450, and 550 m. To collect enough CH_4 for radiocarbon measurements, the entire headspace was extracted and combined in two distinct, pooled samples. One of these pooled samples comprised headspace gases from depths of 105, 112, 118, 130, 140, 160, and 200 m, and the other from 250, 350, 450, and 550 m. The CH_4 was then prepared for radiocarbon analyses as previously described by Kessler & Reeburgh (2005). The samples were analyzed using ^{14}C-Accelerator Mass Spectrometry at the University of California, Irvine.

The pH of the water column was determined on individual samples transferred to plastic bottles without headspace gas using a hand held pH-meter (VWR, West Chester, PA, USA) and an Accumet (Cole-Parmer, Vernon Hills, IL, USA) combination electrode calibrated with three NIST-traceable buffers at the ambient surface water temperature (~29.5 °C). The electrode diameter was adjusted with a piece of Tygon tubing and Parafilm to form an air-tight seal upon its insertion in the sampling bottles. Speciation and saturation state calculations were carried out using the JCHESS geochemical modeling software and the Chess thermodynamic database (van der Lee, 1993).

Microbiology

Samples of cellular material were collected from 2 L of water on 0.45 μm glass fiber filters and preserved at −80 °C. DNA was extracted from these filters using a Mo-Bio PowerSoil extraction kit (MO BIO Laboratories, Carlsbad, CA, USA). 16S rDNA was amplified using polymerase chain reaction (PCR) with Platinum®Taq DNA polymerase and primers designed to target specific groups (Table 1). All PCR cycles were performed according to the specifications given by Invitrogen (Carlsbad, CA, USA) for Platinum®Taq DNA polymerase. To test the reliability of the PCR reactions, positive and negative controls were conducted for each primer set with the exception of the ANME. The PCR products were imaged by gel electrophoresis to check for the positive amplification of the template and to estimate the length of the amplified fragments. The amplified DNA was cloned into the TOPO cloning vector and transformed into chemically competent One Shot TOP10 *E. coli*. Individual clone colonies were randomly selected for sequencing after blue-white β-galactosidase screening to confirm positive ligation. Plasmid

Table 1 Primers used for PCR amplification of DNA

Primer	Sequence (5′–3′)	Target	Reference
EelMS932r	AGCTCCACCCGTTGTAGT	ANME-2	Boetius *et al.* (2000), Lloyd *et al.* (2006)
MethT2r	CATCTCTGRCSAYCATACCGG	Type-2 methanotrophs	Wise *et al.* (1999)
MethT1df	CCTTCGGGMGCCGACGAGT	Type-1 methanotrophs	Wise *et al.* (1999)
MethT1br	GATTCYMTGSATGTCAAGG	Type-1 methanotrophs	Wise *et al.* (1999)
ANMEf	GGCTCAGTAACACGTGGA	ANME-1,2,3	Schubert *et al.* (2006)
915r	GTGCTCCCCCGCCAATTCCT	Archaea	Delong (1992)
27f	AGAGTTTGATCCTGGCTCAG	Bacteria	Lane (1991)
1492r	GGTTACCTTGTTACGACTT	Universal	Lane (1991)
21fa	TTCCGGTTGATCCYGCCGGA	Archaea	Delong (1992)

DNA was purified using a PureLink Quick plasmid Miniprep Kit (Invitrogen, Carlsbad, CA, USA). Forward and reverse sequencing of the purified DNA was performed by Macrogen (Rockville, MD, USA). The number of clones sequenced is presented in Table 3.

Contiguous sequences were assembled using the assembly function in Geneious® (Auckland, New Zealand). BLAST (Basic Local Alignment Search Tool) queries identified all clones generated with amplicons from primers designed to target Type-1 aerobic methanotrophs as similar to *Thiobacillus* sp. Species of the genus *Thiobacillus* are not known aerobic methanotrophs but are known to yield false-positive amplicons with the primer set used (Wise *et al.*, 1999). Phylogenetic analyses of these sequences confirm their classification within the beta-proteobacteria (see phylogenetic tree in Fig. SI11, Appendix 4). These clones were not considered further. Amplicons generated using the Archaeal and ANME-1,2,3 targeting primer sets were also cloned and sequenced. Chimeric sequences in this library were identified with Bellerophon (v.3) and eliminated from the dataset (DeSantis *et al.*, 2006). Nearest non-chimeric neighbors and isolates were identified using Simrank and included in subsequent phylogenetic analyses. Additional sequences were culled from the Greengenes database (Hugenholtz taxonomy) (DeSantis *et al.*, 2006). Sequence alignments were performed using the MUSCLE plugin in Geneious®. Phylogenetic trees were constructed by neighbor joining, maximum likelihood, and Bayesian inference methods using the Geneious tree builder, and the PHYML (Guindon & Gascuel, 2003) and MrBayes (Huelsenbeck & Ronquist, 2001) plugins, respectively. Branching topologies in the neighbor joining and maximum likelihood trees were verified by conducting 1000 and 100 bootstrap analyses, respectively. Lake Matano clone sequences were submitted to GenBank (accession numbers: HM583588–HM583606).

RESULTS

Physical properties of Lake Matano

From 2004 to 2007, Lake Matano remained stratified with a persistent pycnocline between 100 and 120 m depth and non-persistent (seasonal) pycnoclines in the upper 100-m surface layer (Fig. 2) (Crowe *et al.*, 2008b; Katsev *et al.*, 2010). The persistent pycnocline largely results from a decrease in water temperature with increasing depth and is marginally enhanced by higher solute concentrations in the bottom waters. It persists over at least decadal and likely much greater time scales, seemingly unaffected by seasonality (Fig. 2, inset) (Crowe *et al.*, 2008b; Katsev *et al.*, 2010). The seasonal pycnocline was located between 60 and 90 m depth in July 2006, and between 30 and 60 m in February 2007 (Fig. 2). The density gradient in this seasonal pycnocline is largest during the rainy season (February) and is completely eroded by the middle of the dry season (September), likely as a result of evaporative cooling of the surface waters (Crowe *et al.*, 2008b; Katsev *et al.*, 2010). A third, diurnal pycnocline often forms within the upper 30 m as a result of surface water heating by solar radiation (not seen in

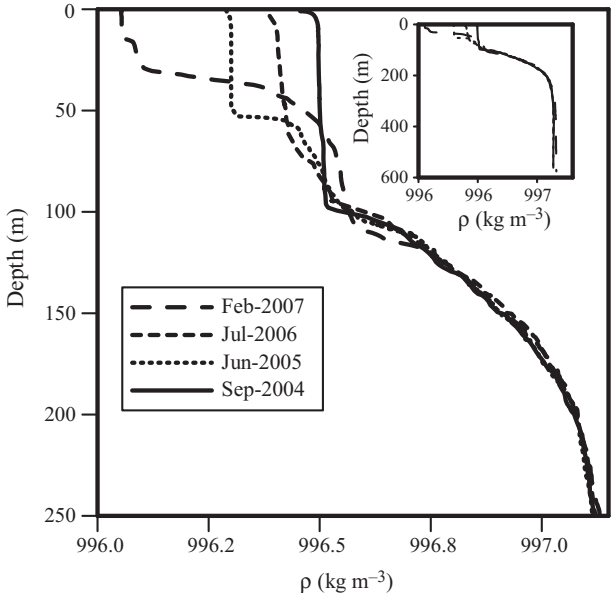

Fig. 2 Representative density profiles from September 2004, June 2005, July 2006, and February 2007 illustrating fluctuations in the seasonal pycnocline within the upper 100 m of the water column. The inset presents the entire water column and shows the consistency of the persistent pycnocline between seasons and over several years.

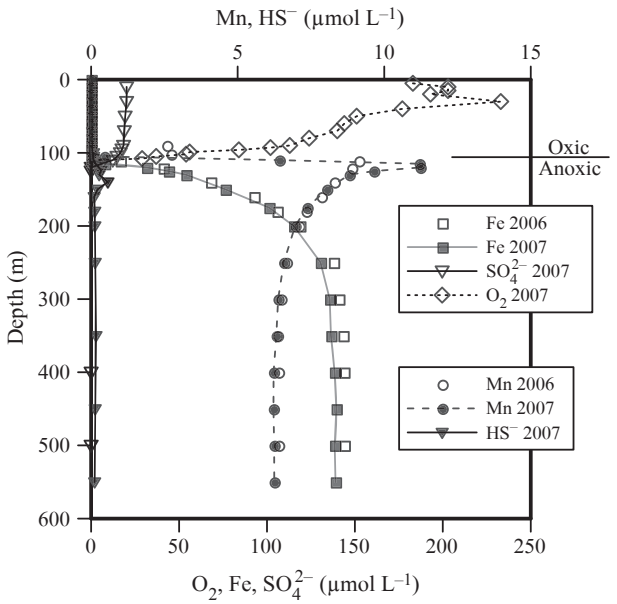

Fig. 3 Depth distribution of major redox active species. In the figure, Fe represents total dissolved Fe, which is equivalent to dissolved Fe(II) (Crowe *et al.*, 2008b). Similarly, HS^- represents concentrations of total dissolved $S(II)^{2-}$ which are an order of magnitude or more greater than the free HS^- concentrations (Crowe *et al.*, 2008a).

the profiles shown in Fig. 2). Thermal profiles, recorded between 2004 and 2007 at numerous locations throughout the lake (not shown), failed to detect a deep heat source, and provide no evidence for hydrothermal activity.

Distributions of major redox active species

The persistent stratification is reflected in the distribution of several redox active species (Figs 3 and 7A). DO in the surface waters was nearly at saturation with respect to the atmosphere and decreased with depth. Hypoxic conditions (<62.5 μmol L^{-1} O_2) (Diaz & Rosenberg, 1995) prevailed between 95 and 110 m, and sub- to anoxic conditions were reached below 110 m. Based on the bathymetry of Lake Matano (Crowe *et al.*, 2008b), the anoxic basin covers 107 km^2 and contains 35 km^3 of anoxic water.

The vertical distributions of other redox active species (Mn, Fe, SO_4^{2-}, and HS^-) were consistent with their respective chemical properties. There was some overlap between dissolved Mn and O_2 within the hypoxic zone: Mn was detected (0.45 μmol L^{-1}) at 105 m depth where O_2 concentrations of up to 37 μmol L^{-1} were measured. The coexistence of these two species in the water column is consistent with the metastability and relatively slow oxidation kinetics of Mn(II) in the presence of O_2 (Luther, 2005; Morgan, 2005). In contrast, Fe was undetectable (<0.1 μmol L^{-1}) within the hypoxic zone but measurable (0.29 μmol L^{-1}) at 110 m, the depth at which O_2 became undetectable (<2.5 μmol L^{-1}). Sulfate concentrations in the surface mixed layer were low (<20 μmol L^{-1}), and trace sulfide (peak of <0.6 μmol L^{-1} at ~140 m; Fig. 3) was detected in the anoxic bottom water. Nitrate and nitrite were undetectable (<100 nmol L^{-1}) within the water column with the exception of a small peak (~200 nmol L^{-1}) of NO_3^- between 90 and 100 m depth (Fig. 4A). Particulate Fe and Mn concentrations also peaked near the persistent pycnocline (Fig. 4B). Nearly identical vertical distributions of these redox sensitive species between 2004 and 2007 (Crowe *et al.*, 2008b) illustrate the near steady-state nature of redox cycling within the pycnocline of Lake Matano. Importantly, the profiles of Fe(II) and NH_4^+ reveal that they originate from the sediment and/or deep bottom waters (i.e., below 200 m where the concentration profiles are vertical), likely due to the anaerobic degradation of organic matter (Katsev *et al.*, 2010).

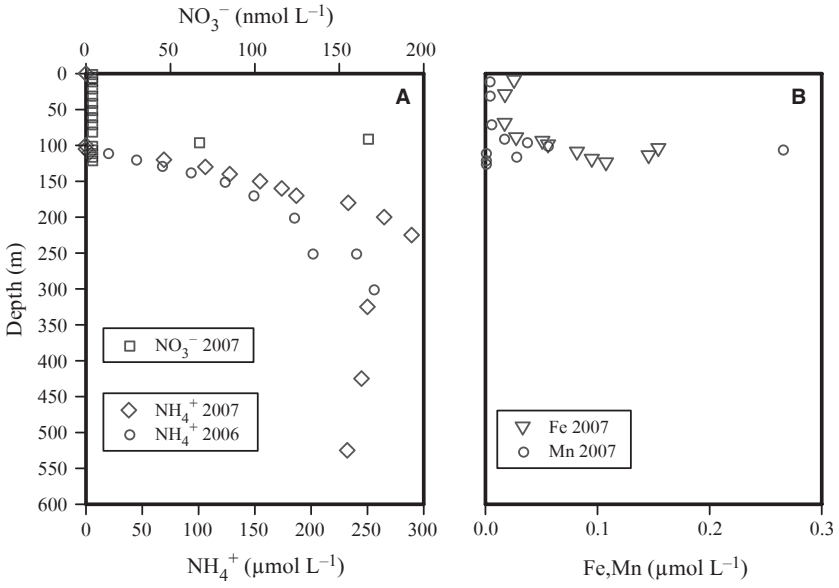

Fig. 4 (A) Depth distribution of NO_3^- (February 2007) and NH_4^+ (July 2006 and February 2007); (B) depth distribution of particulate Fe and Mn (February 2007).

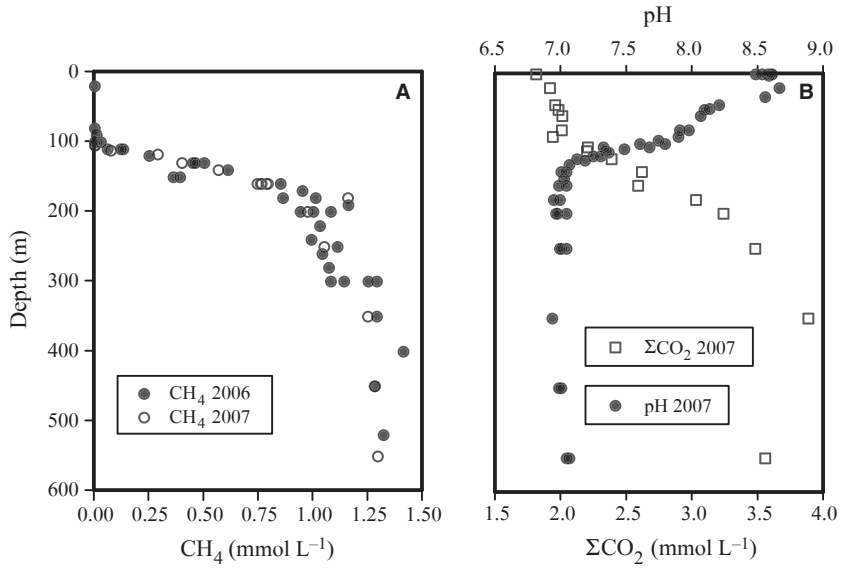

Fig. 5 (A) Depth distribution of CH_4 in July 2006 and February 2007; (B) depth distribution of ΣCO_2 and pH in February 2007. Note that ΣCO_2 was computed from measurements of alkalinity and pH (see text for details).

Without sediment porewater profiles, we cannot distinguish between the two potential sources. Given the highly active regional tectonics and the close proximity of volcanic activity, we had previously postulated a hydrothermal source for Fe(II) but, as pointed out above, we find no evidence for local hydrothermal activity in our vertical temperature profiles.

Distributions of dissolved CH_4 and ΣCO_2

Methane concentrations in Lake Matano ranged from 0.003 mmol L^{-1} in the surface mixed layer to 1.4 mmol L^{-1} in the anoxic bottom water (Fig. 5A): the 35 km^3 anoxic basin of Lake Matano contains 4.6×10^{10} mol or 7.4×10^5 metric tons of CH_4. In comparison, the world's largest anoxic basin, the Black Sea (545 000 km^3), contains 9.6×10^7 metric tons of CH_4 (Reeburgh *et al.*, 1991), but at concentrations less than 0.012 mmol L^{-1} (Schubert *et al.*, 2006). Vertical profiles of methane concentrations constructed from samples taken in both 2006 and 2007 (Fig. 5A) are nearly identical, suggesting that CH_4 concentrations are close to steady state, as are other redox active species (Crowe *et al.*, 2008B). At 0.003 mmol L^{-1}, CH_4 in the surface water is supersaturated with respect to the atmosphere, thus the lake acts as a net source of CH_4 (methane in the surface water diffuses out) to the overlying atmosphere. Below 200 m depth, the concentrations are equivalent to the solubility limit of CH_4 in water at atmospheric pressure (Henry's law constant = 1.3×10^{-3} mol L^{-1} atm^{-1}; Canfield *et al.*, 2005). Hence, samples collected from below 200 m may have degassed during recovery, and actual concentrations may be higher than reported.

ΣCO_2 profiles (computed from total alkalinity and pH measurements using CO_2SYS; Lewis & Wallace, 1998) are given in Fig. 5B. The ΣCO_2 concentrations calculated from the alkalinity measurements are in agreement with measured ΣCO_2 concentrations (data not shown), but the former carry smaller analytical uncertainties. The concentrations of $CO_{2(aq)}$ in the bottom water of Lake Matano are less than 1 mmol L^{-1} (partial pressures up to 0.023 atm) and well below saturation at *in situ* temperatures and pressures (~19 atm at 200 m depth; Table 2). The total partial pressure of gases in the bottom waters did not exceed 5.2% of saturation at the *in situ* temperatures and pressures (Table 2), rendering limnic eruption unlikely.

Table 2 Gas partial pressures and saturation levels

Depth	pH	T	pCH_4	pCO_2†	% Saturation
140	7.00	26.42	0.44	0.014	3.3
160	7.04	26.11	0.61	0.013	4.0
180	6.93	25.89	0.89	0.018	5.2
200	6.95	25.74	0.75	0.019	4.0
250	6.98	25.58	0.81	0.019	3.4
350	6.92	25.49	0.96	0.023	2.9
450	6.96	25.48	0.98	0.023	2.3
550	7.04	25.47	1.00	0.023	1.9

Henry's Law constants (mol L^{-1} atm^{-1}) for CH_4 (1.3×10^{-3}) and CO_2 (3.4×10^{-2}) from Canfield *et al.* (2005).
†ΣCO_2 calculations were made with CO_2SYS (Lewis & Wallace, 1998).

Isotopic data and radiocarbon dating

The C isotopic signature of CH_4 ($\delta^{13}C_{CH4}$) in the deep bottom water was less than −70‰ (Fig. 6A). $\delta^{13}C_{\Sigma CO2}$ values varied between −7‰ and −8‰ throughout most of the water column except for negative excursions to nearly −10‰ both at 104 and 122 m depth (Figs 6 and 7B). The radiocarbon content of CH_4 ($^{14}C_{CH4}$) in the transition zone (depths 105–200 m) was 77.4 ± 0.2 percent Modern Carbon (pMC), whereas it was 75.0 ± 0.1 pMC in the deep water (>250 m

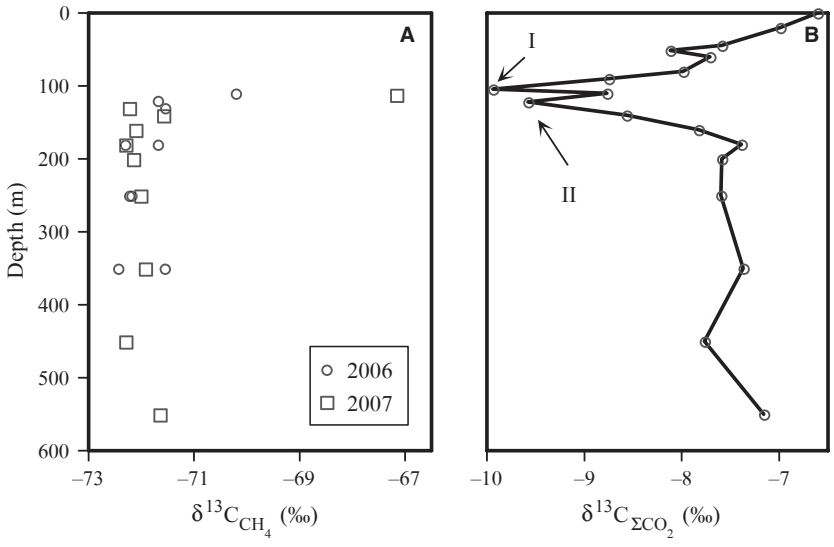

Fig. 6 (A) C isotopic composition of CH_4 in July 2006 and February 2007; (B) C isotopic composition of ΣCO_2 in February 2007. Note that the roman numerals (I and II) in panel B denote the two peaks in $\delta^{13}C_{\Sigma CO2}$.

depth) (Stuiver & Polach, 1977). Measurements of $^{14}C_{CH4}$ yielded conventional (not corrected for reservoir effects) ages of 2043 ± 4 and 2255 ± 5 year before present (BP) for carbon in CH_4 from the transition zone (105–200 m) and deep waters (>200 m), respectively. Thus, the age of the CH_4 accumulating in the deep water is relatively young. If some of the CH_4 were produced from the reduction of hydrothermal ΣCO_2, this methane would not contain ^{14}C and could yield a deceivingly old age for the CH_4 itself. The young age suggests that ancient or distant sources are unlikely. It should be noted that methane might also originate from percolating groundwater, as it may at one of the rare and narrow lake beaches (i.e., Butterfly beach, which is situated on a large block of variably metamorphosed carbonate rocks on the south shore of Lake Matano, Fig. 1).

Microbial ecology

To obtain a preliminary characterization of the microbial community related to methane cycling in Lake Matano, we conducted culture-independent 16S rRNA gene cloning using primers designed to target specific groups (Table 1). Table 3 shows the results of PCR amplification using these primer sets. PCR failed to amplify DNA from known aerobic methanotrophs, indicating that they were absent from the water column or too small to be captured by our 0.45 μm pore-size filters. Phylogenetic analyses of Archaeal amplicons were conducted, and a maximum likelihood tree is shown in Fig. 8. This tree illustrates the phylogenetic relationships between the Lake Matano sequences, other sequences closely related to the Lake Matano clones, and sequences from CH_4-rich environments. Clone sequences, obtained with primers purportedly targeting ANME-1, 2, and 3 (MWC118AM), cluster within the order Methanomicrobiales and are not closely affiliated with any of the ANME. Other studies have also found that the ANME-F primer can lack specificity for

Table 3 Results from PCR amplifications with group-specific primers

Primer set	Target organisms	Sample depth	Amplicon	No. of clones sequenced
MethT1df-MethT1br	Type-1 methanotrophs	140	–	
		120	–	
		118	+	10
		115	–	
		105	+	10
MethT2r-27f	Type-2 methanotrophs	140	–	
		120	–	
		118	–	
		115	–	
		105	–	
21fa-915r	Archaea	140	–	
		120	+	0
		118	+	50
		115	–	
		105	–	
ANMEf-915r	ANME-1, 2, 3	118	+	10
21fa-EelMS932r	ANME-2	118	–	

known ANME (Schubert *et al.*, 2006). Clone sequences MWC118AM 2, 3, 4, 7, 8, 9, and 10 cluster tightly with each other and with additional clones obtained with primers targeting Archaea in general (MWC118AR 3, 8, 10, 14, and 11) (Fig. 8). Isolated organisms most closely related to these clone sequences are known methanogens of the family Methanomicrobiaceae, which use either hydrogenotrophic CO_2 reduction or formate disproportionation to generate methane. One other clone, MWC118AR clone 7, clusters within the order Methanosarcinales and is closely related to known methanogens of the family Methanosaetaceae. The remaining Archaeal clone sequences are widely distributed within the kingdom Crenarchaeota (data not shown). Many of the previously isolated Crenarchaeota that are closely related to these Matano clones are deeply rooted and thermo-

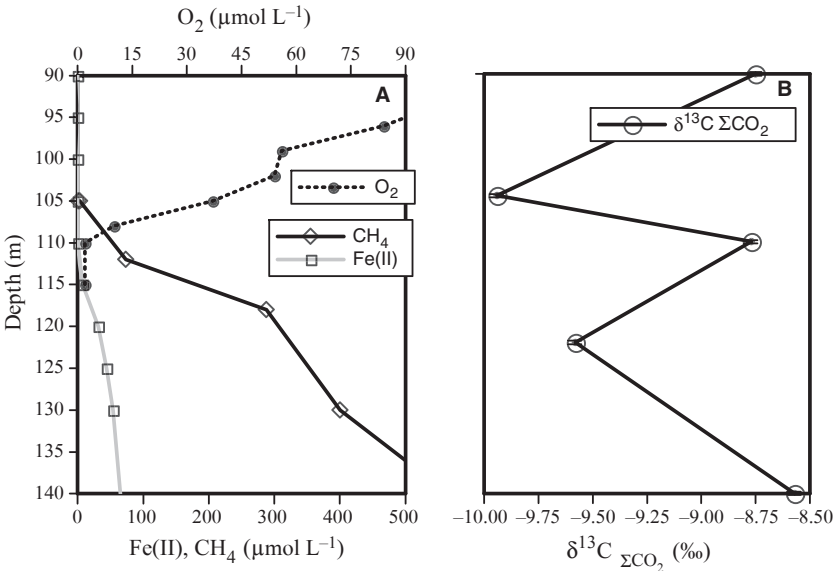

Fig. 7 (A) Chemical profiles within the vicinity of the persistent pycnocline, illustrating the overlap, or lack thereof, between species in the zone of methane oxidation; (B) C isotopic composition of ΣCO_2 in February 2007, error bars are 0.1‰ (analytical precision) and fit within the symbol.

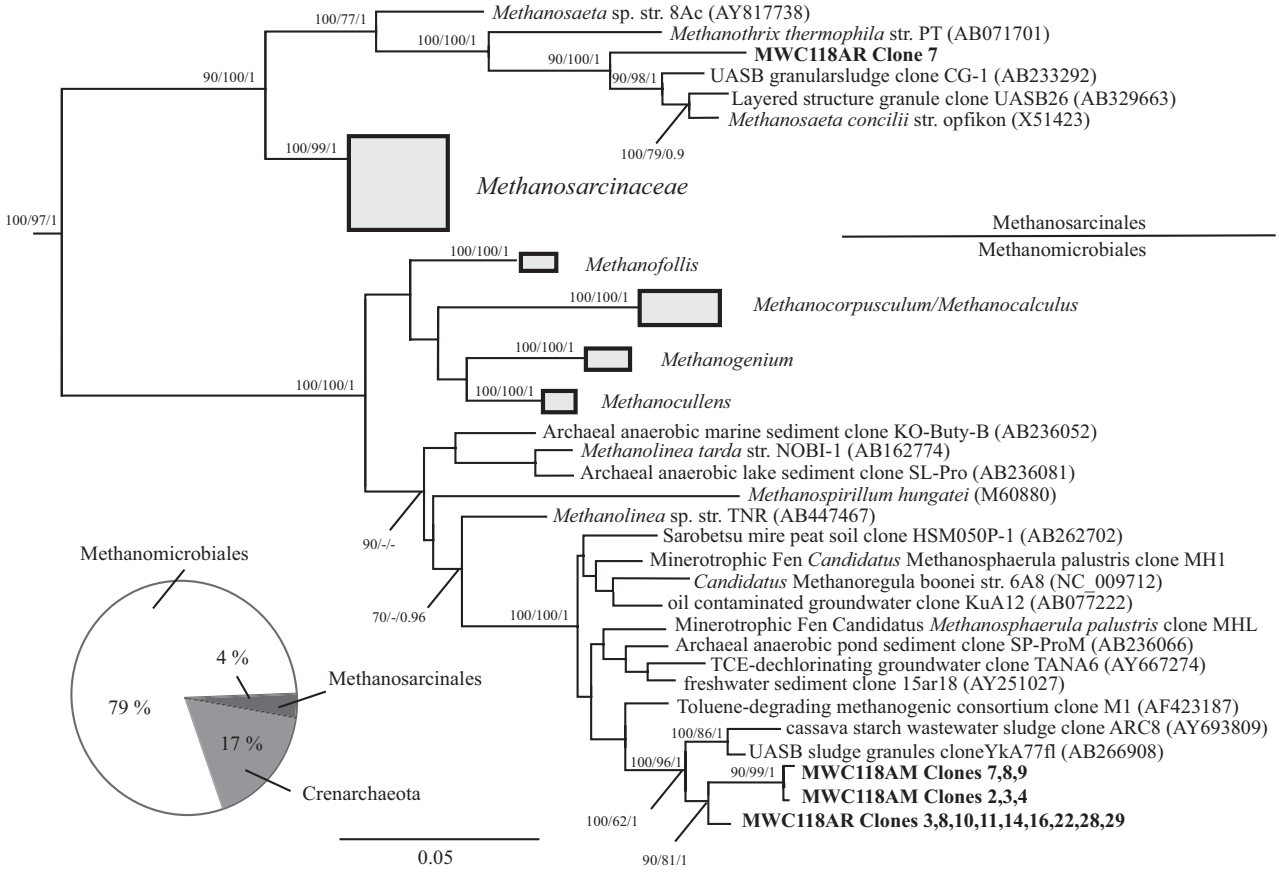

Fig. 8 Phylogenetic tree displaying the affiliations of 16S rRNA sequences obtained from 118 m depth in Lake Matano using both PCR primers to target Archaea in general (MWC118AR) and the ANME (MWC118AM). The tree includes reference species in addition to clones obtained from methane-rich environments and the nearest non-chimeric neighbors identified using the Greengenes Simrank tool. The tree was constructed using the PHYML Maximum Likelihood algorithm. The numbers at the branching nodes represent bootstrap support for neighbor joining (1000 bootstrap replications) and maximum likelihood (100 bootstrap replications) in addition to probability from Bayesian inference (NJ/ML/BI). Bootstrap support of less than 60% and probabilities of less than 0.6 are not shown. The clone sequences from Lake Matano are emphasized with a bold font. *Aquifex pyrophilus* (M83548) was used as an outgroup to root the tree. The inset shows the distribution of the main Archaeal phylotypes as a percentage of the number of clones sequenced.

phyllic. Of the clones sequenced from DNA amplified with the general Archaeal primers, 79% belonged to the order Methanomicrobiales, 4% to the order Methanosarcinales, and the remaining 17% were Crenarchaeota. It is noteworthy that our PCR with Archaeal primers failed to generate products at depths of 105, 115, and 140 m. It is possible that the PCR reaction was possibly inhibited for these samples, but our ability to amplify bacterial DNA argues against this. Alternatively, Archaeal cell abundances may have been lower in water from these depths.

DISCUSSION

According to the vertical distribution of CH_4 in the water column of Lake Matano (Fig. 5A), net CH_4 production occurs in the sediments or bottom waters, whereas net CH_4 consumption occurs within the 100–200 m depth interval. The sharp methane concentration gradient between 200 and 100 m depth implies the presence of a methane sink in the vicinity of the persistent pycnocline. In the following discussion, we constrain the rates and pathways of CH_4 production and consumption to develop a mechanistic understanding of CH_4 cycling in Lake Matano.

Methane production pathway

The carbon isotopic composition of CH_4 ($\delta^{13}C_{CH4}$) (less than −70‰) clearly demonstrates its biological origin (Whiticar, 1999). This biogenic CH_4 has accumulated to relatively high concentrations despite the abundance of Fe and Mn (hydr)oxides, which, according to thermodynamic arguments, should preclude methanogenesis (Reeburgh, 2007). Standard-state thermodynamic calculations, however, ignore bioavailability and the kinetics of substrate uptake (Roden & Wetzel, 2003). For example, Roden (2003) suggested that the capacity of microbial Fe(III) oxide reduction to suppress other terminal electron acceptor pathways in anoxic soils and sediments is controlled by the reactive (i.e., microbially accessible) surface site density rather than the thermodynamic properties of the bulk (hydr)oxide minerals. Accumulation of sorbed and/or surface-precipitated Fe(II) on Fe(III) (hydr)oxide surfaces renders these surfaces progressively inaccessible to Fe-reducing bacteria and, thereby, alters the long-term reactivity of Fe(III) (hydr)oxides (Roden & Urrutia, 1999, 2002). Given the high concentrations of dissolved Fe(II) in the anoxic bottom waters (Fig. 3) and sediment porewaters (Fowle *et al.*, 2006) of Lake Matano, surface deactivation of Fe(III) (hydr)oxides that sink through the bottom waters and accumulate in the lake sediments in high abundances (up to 20 wt.%; Crowe *et al.*, 2004) is plausible. Furthermore, the absence of bioturbation in the anoxic bottom sediments limits recycling and regeneration of reactive Fe (hydr)oxide surfaces, promoting methanogenesis relative to Fe reduction (Roden & Wetzel, 1996).

The difference between the carbon isotopic compositions of methane and ΣCO_2 in the deep anoxic bottom waters yields an isotope separation factor (ε_C), which is commonly used to fingerprint the different methanogenic pathways (Whiticar, 1999). The ε_C in Lake Matano, ~65‰, is within the range of fractionation factors observed for pure cultures of methylotrophic and hydrogenotrophic methanogens and is much higher than the 24–27‰ observed in pure cultures of acetate disproportionating organisms (Whiticar, 1999). Hence, this large isotope separation factor may indicate that CH_4 production in Lake Matano is dominated by hydrogenotrophic methanogens. This is broadly consistent with the microbial ecology of the water column, which identifies most of the methanogen clone sequences as members of the order Methanomicrobiales. The Methanomicrobiales isolated to date utilize H_2/CO_2, formate, and alcohols as substrates, and they are not known to conduct acetate disproportionation (Canfield *et al.*, 2005). Nevertheless, there is some disparity between the true fractionation factors observed in culture-based experiments and the isotope separation factors observed in natural systems dominated by one form of methanogenesis or another. Given that the Lake Matano ε_C value falls at the very upper end of those observed in systems dominated by acetate disproportionation and at the lower end of values reported for systems dominated by CO_2 reduction (Whiticar, 1999), methanogenesis in Lake Matano may occur via both pathways. Indeed, the water column clone MWC118AR 7 groups within the Methanosaetaceae and all known Methanosaetaceae are obligate acetate disproportionators (Canfield *et al.*, 2005). A more detailed microbiological study will be needed to resolve the specific methanogenic pathways in Lake Matano.

Regardless of the specific pathway, the presence of methanogens within the chemocline of Lake Matano indicates that methanogenesis may occur directly within the water column, despite the fact that the concentration profiles implicate the sediment as the principal CH_4 source. DNA sequences and biomarkers affiliated with methanogens have been detected in the water column of the Black Sea (Vetriani *et al.*, 2003; Schubert *et al.*, 2006). Due to the high abundance of sulfate in the Black Sea water column, it was concluded that these methanogen signatures originated from anaerobic methane oxidizing Archaea and that methanogenesis was not operating directly in the water column. A similar argument could be made with respect to Fe in the water column of Lake Matano, and this is discussed below (see next section). Though measured in the water column of a meromictic lake (Iversen *et al.*, 1987), water column methane production appears to be rare in modern anoxic water columns (Reeburgh, 2007). Lake Matano provides a new environment in which to study pelagic methanogenesis under persistently anoxic conditions.

We also note that most of Lake Matano's Euryarchaeota water column clones cluster tightly with each other (Fig. 8), and their closest isolated relatives belong to newly described

genera of the order Methanomicrobiales, including *Methanolinea* (Imachi *et al.*, 2008), *Methanoregula* (Brauer *et al.*, 2006a), and *Methanosphaerula* (Cadillo-Quiroz *et al.*, 2009). Our clones, the aforementioned isolates and additional clone sequences, form a coherent clade previously referred to as the 'R-10 or Fen cluster' (Brauer *et al.*, 2006b). This clade is clearly separated (bootstrap support of 100 for neighbor joining and maximum likelihood trees, and a probability of 1 for the Bayesian tree) from the other families of the Methanomicrobiales, and our work extends the environmental distribution of the R-10/Fen cluster from wetlands and wastewater sludges to stratified, freshwater lakes.

Methane oxidation pathway(s)

Methane oxidation in aquatic environments is catalyzed by bacteria and Achaea (Reeburgh, 2007; Bastviken *et al.*, 2008). Microbial CH_4 oxidation is known to occur both aerobically (i.e., with O_2) and anaerobically with either SO_4^{2-} (Hinrichs *et al.*, 1999; Boetius *et al.*, 2000; Orphan *et al.*, 2001) or NO_3^- (Raghoebarsing *et al.*, 2006; Ettwig *et al.*, 2008) as the electron acceptor. Sulfate-dependent anaerobic oxidation of methane (AOM) is responsible for most CH_4 oxidation in marine sediments (Strous & Jetten, 2004) where it consumes more than 90% of the CH_4 produced (Reeburgh, 1996; Knittel & Boetius, 2009). As lake water sulfate concentrations are typically low, lakes emit globally more methane to the atmosphere than the ocean, and they are responsible for between 6 and 16% of total non-anthropogenic methane emissions (Bastviken *et al.*, 2004). AOM coupled to denitrification has been observed in laboratory cultures (e.g. Ettwig *et al.*, 2008), but its environmental significance is unknown. Under standard state, AOM with the (hydr)oxides of Fe and Mn is thermodynamically favorable, but conclusive evidence for Fe- or Mn- dependent AOM in the environment remains elusive (Zehnder & Brock, 1980; Gal'chenko, 2004; Konhauser *et al.*, 2005; Nauhaus *et al.*, 2005; Caldwell *et al.*, 2008; Beal *et al.*, 2009). Recently, Mn- and Fe- dependent AOM was postulated in laboratory incubations of S-poor marine sediments (Beal *et al.*, 2009), but the results of this study do not constrain the role of Fe and Mn (hydr)oxides in methane oxidation. As noted by the authors, SO_4^{2-} may have been regenerated through the oxidation of sulfide coupled to reduction of the added Fe and Mn (hydr)oxides. In Lake Matano, the dearth of SO_4^{2-} (Crowe *et al.*, 2008a,b) and NO_3^- might preclude AOM, but rapid cycling of Fe and Mn within the chemocline may allow CH_4 oxidation to take place through Fe(III) or Mn(III/IV) reduction. We consider this possibility in detail below.

A sharp gradient in the methane concentration (Fig. 5) between 100 and 200 m depth implies that methane oxidation occurs at or immediately below the persistent pycnocline. The oxidation of isotopically light, biogenic CH_4 should be reflected in the C isotopic composition of its oxidation product, ΣCO_2. This is supported by our data, which show two distinct minima in the $\delta^{13}C_{\Sigma CO2}$ (points I and II in Fig. 6B) profile at depths of 104 and 122 m that, together, delineate the depth interval of methane oxidation. Similarly, heavier CH_4 ($\delta^{13}C_{CH4}$ shifted to less negative values) is observed between 110 and 115 m (Fig. 6A). The concentrations of methane and ΣCO_2 in the deep water are such that a complete oxidation of methane to CO_2 would produce a $\delta^{13}C_{\Sigma CO2}$ as low as $-23‰$. The more positive values observed likely reflect a combination of dilution by heavier epilimnetic and deep water ΣCO_2 and the escape of a small fraction of CH_4 to the atmosphere.

The $\delta^{13}C_{\Sigma CO2}$ values observed at 104 and 122 m and the relatively heavier ΣCO_2 observed at 110 m generates a 'saw-tooth' pattern that can only be explained by sources of isotopically light ΣCO_2 at 104 and 122 m and a sink of isotopically light ΣCO_2 at 110 m (Figs 6B and 7B for more detail). The obvious source for isotopically light ΣCO_2 in the vicinity of the persistent pycnocline is the oxidation of CH_4. The sink for isotopically light ΣCO_2 at 110 m is likely generated by the preferential uptake of $^{12}C_{\Sigma CO2}$ during microbial C fixation or methanogenesis. Indeed, this positive excursion is coincident with the presence of a community of putative photoferrotrophic Chlorobiaceae capable of photosynthetic C-fixation (Crowe *et al.*, 2008a). Regardless of its origin, the sink for isotopically light ΣCO_2 clearly delineates two spatially distinct zones of methane oxidation and calls for a discussion of the potential oxidants available within these zones (see Appendix 1 for a quantitative examination of the C fluxes and the resulting isotope ratios).

The peak in $\delta^{13}C_{\Sigma CO2}$ at point I (104 m, Fig. 6B) likely results from aerobic methane oxidation. Interpolation between O_2 concentrations measured at 102 m (54 μmol L^{-1}) and 105 m (37 μmol L^{-1}) yields an estimated O_2 concentration of 43 μmol L^{-1} at 104 m, which is well above typical half-saturation constants for aerobic methanotrophs (van Bodegom *et al.*, 2001). Oxygen in Lake Matano becomes undetectable (≤2.5 μmol L^{-1}) below 110 m (Figs 3 and 7A), and the peak in $\delta^{13}C_{\Sigma CO2}$ at point II (122 m, Fig. 6B) indicates that CH_4 oxidation occurs in the presence of little or no oxygen. Aerobic methane oxidation below our oxygen detection level may be possible, but it should be kinetically inhibited by the high Fe(II) concentrations (Appendix 2). Our calculations (Appendix 2) reveal that the kinetics of abiotic Fe(II) oxidation at circum-neutral pH is sufficiently rapid that Fe(II) competes with methanotrophic bacteria for molecular oxygen, potentially favoring anaerobic methane oxidation. Based on the known kinetics of aerobic methanotrophy (van Bodegom *et al.*, 2001, 2004) and abiotic Fe(II) oxidation (Millero *et al.*, 1987), the maximum potential rate of aerobic methane oxidation at ~120 m depth is 4.5×10^{-8} mol L^{-1} day^{-1}. This rate is one order of magnitude lower than the methane oxidation rate (5×10^{-7} mol L^{-1} day^{-1}) necessary to sustain the $\delta^{13}C_{\Sigma CO2}$ peak at point II

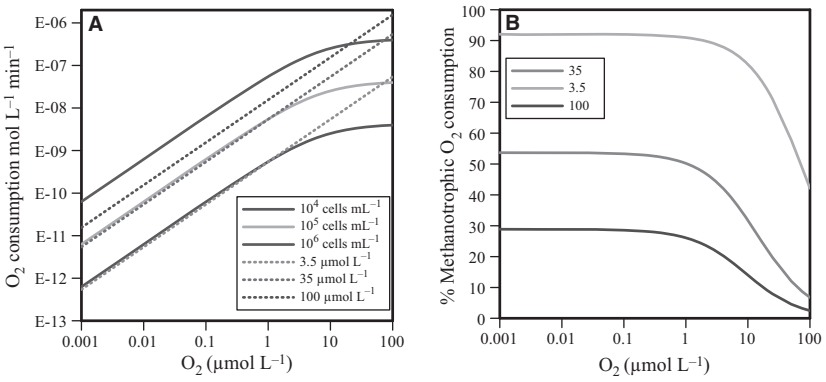

Fig. 9 (A) Rates of O_2 consumption by methanotrophy (solid lines; light gray = 10^4 cells mL^{-1}, dark gray = 10^5 cells mL^{-1}, black = 10^6 cells mL^{-1}) and Fe(II) oxidation (dotted lines; black = 3.5 μmol Fe(II) L^{-1}, dark gray = 35 μmol Fe(II) L^{-1}, light gray = 100 μmol Fe(II) L^{-1}). (B) Percentage of oxygen consumed by aerobic methanotrophy vs. aerobic methanotrophy plus Fe(II) oxidation (cell density = 10^5 cells mL^{-1}, black = 3.5 μmol Fe(II) L^{-1}, dark gray = 35 μmol Fe(II) L^{-1}, light gray = 100 μmol Fe(II) L^{-1}) as a function of DO concentration.

(122 m) against the diffusion of heavier ΣCO_2 (see Appendix 1 for details on the calculation of CH_4 oxidation rates from $\delta^{13}C_{\Sigma CO2}$ profiles). Furthermore, the maximum rate of aerobic methane oxidation calculated in Appendix 2 assumes that aerobic methanotrophic bacteria occur at moderately high cell densities of 10^5 cells mL^{-1}. PCR failed to amplify DNA of known aerobic methanotrophs from cellular material collected at 118 m (Table 3). Unless cellular material was present in the form of very small, free living cells (<0.45 μm) that were not captured on our filters and, thus, overlooked in our genetic assays, the PCR data indicate that the cell density of known aerobic methanotrophs must be very low and the rates of aerobic methane oxidation at and around 122 m depth must be insignificant. Taken together, the available evidence leads us to conclude that some methane oxidation takes place below the depth of oxygen penetration and is, therefore, anaerobic.

Within the depth interval of putative anaerobic methane oxidation in Lake Matano, both sulfate and nitrate occur at exceedingly low concentrations, unlike Fe and Mn (Figs 3 and 4). Methane oxidation coupled to the reduction of Fe or Mn (hydr)oxides is energetically favorable under standard conditions:

$$CH_4 + 8Fe(OH)_3 + 15H^+ \rightarrow HCO_3^- + 8Fe^{2+} + 21H_2O \quad (-572.15\,kJ\,mol^{-1}) \quad (1)$$

$$CH_4 + 4MnO_2 + 7H^+ \rightarrow HCO_3^- + 4Mn^{2+} + 5H_2O \quad (-789.91\,kJ\,mol^{-1}) \quad (2)$$

Reactions 1 and 2 are also favorable over a broad range of environmental conditions, including those encountered within the zone of CH_4 oxidation in Lake Matano (see Appendix 3, Fig. 10). Given the slow oxidation kinetics of CH_4 under most environmental conditions, CH_4 oxidation coupled to Mn or Fe reduction would likely need to be biologically catalyzed. Indeed, sterilized controls failed to elicit methane oxidation activity in incubations of marine sediments, purportedly occurring via the reduction of Fe and Mn (Beal *et al.*, 2009).

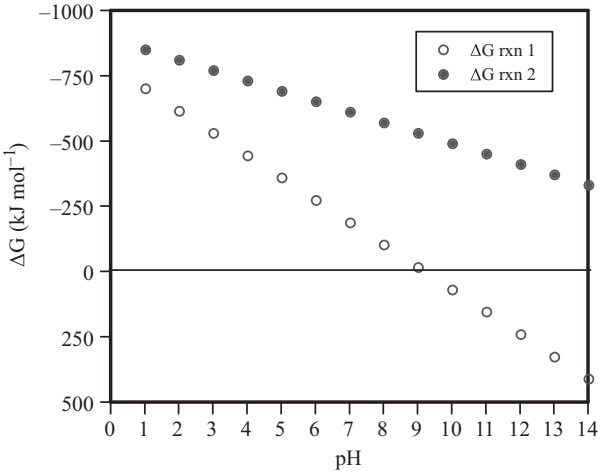

Fig. 10 Free energy yields for reaction 5 (oxidation of CH_4 with $Fe(OH)_3$ as the oxidant) and reaction 6 (oxidation of CH_4 with MnO_2 as the oxidant) at 25 °C, pH = 7.0, Fe^{2+}/Mn^{2+} = 10 μmol L^{-1}, CH_4 = 10 μmol L^{-1}, and HCO_3^- = 1 $mmol^{-1}$. Activity coefficients were assumed equal to 1 for all species.

The minimum energy yield required for organisms to conserve energy for growth from a chemical reaction is thought to be around 15 kJ mol^{-1}, based on ATP generation using four protons per ATP molecule (Caldwell *et al.*, 2008). Given the chemical conditions present at 120 m in Lake Matano, under standard state (25 °C and concentration = activity), reactions 1 and 2 yield free energies of −166.8 and −610.9 kJ mol^{-1}, respectively, well in excess of the minimum microbial energy requirement. Accordingly, both reactions could support microbial growth down to sub-nanomolar CH_4 concentrations under circum-neutral pH conditions, indicating that the pathway could operate in a broad range of sedimentary and soil environments at low CH_4 concentrations (see Appendix 3, Fig. 10). In Lake Matano, AOM coupled to Fe(III) or Mn(III/VI) reduction provides a thermodynamically feasible alternative to highly active aerobic methanotrophs working at the exceedingly low O_2 concentrations encountered near 122 m depth. The following discussion considers the rates of CH_4 oxidation and Fe(III) and Mn(III/IV) supply in the pycnocline region.

The sharp Mn(II) and Fe(II) concentration gradients in Lake Matano that are maintained by oxidation drive large fluxes of Mn and Fe near the persistent pycnocline and should generate an abundant supply of both authigenic Fe and Mn (hydr)oxides in the vicinity of point II (Figs 3 and 6B). The Fe(II) concentration gradient between 120 and 110 m (0.003 mol m^{-4}) translates to volume-specific Fe oxidation rates of 5×10^{-8} mol L^{-1} day^{-1}, assuming that oxidation occurs over a 10 m depth interval and a vertical diffusivity of 0.16 m^2 day^{-1} (Katsev *et al.*, 2010). Thus, to generate sufficient authigenic Fe(III) to oxidize 5×10^{-7} mol L^{-1} day^{-1} CH_4 requires that every Fe atom be recycled eighty times within the pycnocline region. Fe and Mn are known to be recycled hundreds of times in bioturbated marine sediments where the activity of macrobenthic fauna mixes reduced Fe and Mn into the oxic layers of the sediment (Canfield *et al.*, 1993). In Lake Matano, such recycling could be achieved through the upward flux of Fe(II) and Mn(II), their oxidation at the oxycline, and a return flux of particulate Fe(III) and Mn(III/IV). Alternatively, photosynthetic Fe oxidation (photoferrotrophy) could regenerate Fe(III) anaerobically. Such a tightly coupled Fe-CH_4 cycle, whereby photogenic Fe (hydr)oxides are rapidly reduced during CH_4 oxidation, could account for the apparent lack of particulate Fe(III) in the vicinity of the persistent pycnocline. Similar arguments could be made for Mn cycling. However, to our knowledge, phototrophic Mn oxidation has never been documented. Another possibility is that short-lived events, such as heavy rainfalls, which were missed by our discrete sampling intervals, deliver pulses of particulate material from the catchment soils to the water column. These events could supply Fe(III) and Mn(VI) intermittently to the chemocline and fuel episodic methane oxidation. A preliminary examination of the chemistry of Fe in the lateritic catchment soils reveals that these soils contain up to 25 wt.% ascorbate-extractable Fe (A. Mucci and S. A. Crowe, unpublished data), and a significant portion of the Fe washed into the lake would be available for microbial reduction.

We can also estimate the total rate of Fe supply to the lake based on a sedimentary Fe content of 20 wt.% (Crowe *et al.*, 2004) and a deepwater sedimentation rate of 0.08 cm $year^{-1}$ (Crowe *et al.*, 2004). Sediment water contents of 90% and a particle density of 2.97 g cm^{-3} (S. A. Crowe, unpublished data) translate to an Fe burial rate of 8.5×10^{-3} mol m^2 day^{-1}, a factor of 5 greater than the upward flux of CH_4 (1.6×10^{-3} mol m^{-2} day^{-1}, see next section). These Fe burial rates reveal that AOM coupled to Fe-reduction could account for a maximum of 66% of total methane oxidation, based on the stoichiometry of reaction 1. The amount of Fe available for CH_4 oxidation would also depend on its reactivity towards microbial reduction and on competition with microbes using Fe(III) as an electron acceptor in organic matter oxidation. Due to the sparseness of the sediment data, these estimates should be taken as preliminary. They also assume no recycling of Fe(III), which could increase the amount of CH_4 oxidized via Fe(III).

The rates we calculate for AOM in Lake Matano (5×10^{-7} mol L^{-1} $days^{-1}$, See Appendix 1 for calculations) are lower than the rates of alleged Fe- and Mn-dependent AOM observed in marine sediment incubations (Beal *et al.*, 2009). Thus, the Fe- and Mn-reducing, methane-oxidizing micro-organisms in Lake Matano appear to operate at rates consistent with the observed physiological capabilities of other such putative organisms. A lack of phylogenetic affiliation between our clone sequences and the ANME does not rule out AOM, and the phylogenetic distribution of methane-oxidizing Archaea may extend beyond known ANME. Furthermore, the micro-organisms involved in NO_3^--dependent AOM are not closely related to the ANME (Raghoebarsing *et al.*, 2006) and may be exclusively bacterial (Ettwig *et al.*, 2008). A similar explanation was put forth to account for decreases in the relative abundance of ANME as a function of incubation time in laboratory experiments with marine sediments (Beal *et al.*, 2009). Further resolving the rates and pathways of CH_4 oxidation in Lake Matano will require measurements of gross CH_4 oxidation rates, gross rates of anoxygenic photosynthesis, organism culturing, and better vertical sampling resolution.

Balancing carbon budgets

The concentration profiles of CH_4 observed in 2006 and 2007 were identical within the precision of our sampling and analyses. Hence, the CH_4 cycle in Lake Matano is at steady state over the time scale of our observations. At steady state, the rate at which methane is supplied from the sediments and deep waters equals the rate at which it is oxidized in the vicinity of the persistent pycnocline. The latter can be estimated from the fluxes of methane between 200 and 100 m depth. Using an average vertical diffusion coefficient of 0.16 m^2 day^{-1}, estimated from the Brunt-Väisälä stability frequency (Crowe *et al.*, 2008b; Katsev *et al.*, 2010), and a methane concentration gradient of 9.7×10^{-3} mol m^{-4} between 200 and 100 m depth, our calculation yields a methane oxidation rate of 1.6×10^{-3} mol m^{-2} day^{-1}. The rates of methane production and methane oxidation in Lake Matano are relatively high and comparable to those observed in the Florida Everglades (King *et al.*, 1990) and freshwater tidal swamps (Megonigal & Schlesinger, 1997). At this rate, methane concentrations in the deep waters would reach the present levels within about 1000 years following a hypothetical mixing event (i.e., overturn). This suggests that the lake has not experienced complete mixing in the last millennium, a time frame consistent with the $^{14}C_{CH4}$ measurements.

The steady-state organic matter degradation rate in Lake Matano was estimated at 3×10^{-3} mol m^{-2} day^{-1}, based on the ammonium concentration gradient (Fig. 4A), an organic matter C:N ratio of 10, and assuming steady-state. The

settling organic matter C:N ratio of 10 was calculated from the ratio of the difference between the ΣCO_2 in the surface and bottom water and the NH_4^+ concentrations in the bottom water. This C:N ratio is consistent with the measured C:N ratio of 12 determined from the elemental analysis of POM recovered from 32 m depth. A comparison of the rates of methanogenesis using the stoichiometries of acetate disproportionation and hydrogenotrophic methanogenesis reveals that 50 or 100%, respectively, of carbon degradation occurs through methanogenesis. Some intermediate value is most likely, given our isotopic data (calculated isotope separation values) and the methanogen ecology. Clearly, methanogenesis and methanotrophy play a key role in Lake Matano's carbon cycle.

Integrated primary production rates in the surface waters (3.8×10^{-3} mol C m^{-2} day^{-1}) (Crowe *et al.*, 2008a) indicate that autochthonous primary production can supply sufficient carbon for the observed rates of organic matter degradation and methanogenesis. The agreement between the computed and measured C:N ratios and a C:N ratio of 49 for allochthonous leaf litter further suggests that respiration and methanogenesis in Lake Matano are largely fueled by autochthonous POM. The difference between the total organic carbon degradation and primary production rates reveals that roughly 78% of the organic matter generated by primary production is degraded, and the rest is buried in the sediment at an approximate rate of 8.4×10^{-4} mol m^{-2} day^{-1}. Lake Matano sediments contain between 5 and 8 wt.% organic carbon, which, given a deep water sedimentation rate of 0.08 cm $year^{-1}$ (Crowe *et al.*, 2004), translates to organic carbon accumulation rates of between 8.5 and 13×10^{-4} mol C m^{-2} day^{-1}, consistent with the above estimate.

The minimum fraction of organic matter degraded through microbial Fe reduction can be estimated by considering the flux of Fe(II) through the pycnocline. Again, we assume that steady state conditions and a diffusion coefficient of 0.16 m^2 day^{-1} apply. The upward flux of Fe(II) is driven by the concentration gradient sustained by Fe(II) oxidation reactions at or near the pycnocline. At steady state, it equals the rate of Fe(II) production via bacterial Fe(III) reduction in the bottom waters and sediments. However, only a fraction of the total Fe(II) produced in the bottom waters and sediments is consumed through oxidation within the pycnocline. Fe(II) is also likely removed by precipitation as siderite ($FeCO_3$), with which the deep waters of Lake Matano are supersaturated, and/or via sorption to sedimentary particles. Fe(II) production rates calculated from the oxidative Fe(II) flux underestimate the total Fe(II) production rates, as they do not include Fe(II) sequestered by precipitation/adsorption. A minimum estimate for the carbon degradation rate by Fe reduction, calculated from the flux of Fe(II) at the pycnocline, is 2.2×10^{-4} mol m^{-2} day^{-1}, less than 10% of the estimated total organic C degradation rate (3×10^{-3} mol m^{-2} day^{-1}) and only 7–14% of the C degraded by methanogenesis (1.6×10^{-3} mol m^{-2} day^{-1}), depending on the pathway considered.

Methane in Fe-rich environments and the Archean Ocean

The prominence of methane in the carbon cycle of Lake Matano demonstrates that methanogenesis and methanotrophy can be viable, and even major, metabolic pathways in ferruginous ecosystems. Although ferruginous ecosystems are rare on the modern earth, Fe-rich, S-poor conditions have dominated ocean chemistry throughout much of Earth's history, particularly during the Archean Eon (Canfield *et al.*, 2006). Geological evidence for the early evolution of methanogens and their activity in ferruginous Archean Oceans (Canfield *et al.*, 2006) is provided by findings of isotopically light carbon in Archean sedimentary kerogens (Hayes, 1983), which is diagnostic of Archaeal methanogenesis and coeval methanotrophy, and CH_4 trapped in fluid inclusions (Ueno *et al.*, 2006). It has been proposed that the lack of C isotopic evidence for methanogenesis and methanotrophy in the carbonate minerals preserved in banded iron formations (BIF) could be a consequence of anaerobic oxidation of CH_4 coupled to Fe reduction (Konhauser *et al.*, 2005). Based on the equilibrium carbon isotope fractionation factor for the siderite-$HCO_3^-{}_{(aq)}$ system ($10^3 \ln\alpha = 0.5 \pm 0.2‰$) (Jimenez-Lopez & Romanek, 2004), the $\delta^{13}C_{\Sigma CO2}$ (−7‰ to −10‰) in the anoxic Lake Matano water column indicates that methanogenesis followed by methane oxidation under ferruginous conditions could yield carbonate minerals with a C isotopic composition of −6‰ to −10‰. Such values are well within the range of −5‰ to −15‰ observed for carbonate minerals in BIFs (Becker & Clayton, 1972; Baur *et al.*, 1985; Konhauser *et al.*, 2005). Hence, the absence of a light $\delta^{13}C$ signature in BIF carbonates does not preclude methanogenesis during BIF diagenesis but may be indicative of anaerobic methane oxidation, possibly coupled to Fe reduction as previously suggested (Konhauser *et al.*, 2005). Though the evidence is mounting, the tenability of such hypotheses clearly rests on a conclusive demonstration of Fe- and Mn-dependent AOM.

CONCLUSIONS

Biogenic CH_4 accumulates in Lake Matano's deep waters to concentrations exceeding 1.4 mmol L^{-1}, amongst the highest recorded in natural waters and comparable to concentrations in lakes receiving volcanic gas inputs, such as Lake Kivu. The sum of the partial pressures of dissolved CO_2 and CH_4 in the bottom waters of Lake Matano does not exceed 6% of the *in situ* hydrostatic pressure. Thus, ebullition at depth is unlikely, and the risk of gas-driven limnic eruptions is low. Despite the abundance of Fe(III) solid phases in Lake Matano, methanogens effectively compete for substrates and are responsible for recycling up to 50% of the C fixed during primary production. Pelagic methanogenesis was confirmed by the presence

of methanogens from the R-10/Fen cluster and of the family Methanosaetaceae within the water column. Given the isotopic compositions of CH_4 and CO_2 and the methanogen ecology, methanogenesis in Lake Matano may occur via both disproportionation of acetate and reduction of CO_2 using H_2 as an electron donor. Upward diffusing CH_4 is oxidized in the vicinity of the persistent pycnocline, and some methane oxidation occurs, seemingly in the absence of O_2, SO_4^{2-}, and NO_3^- but in the presence of Fe and Mn (hydr)oxides. This suggests AOM coupled to Fe or Mn reduction in Lake Matano, but positive identification requires further studies.

ACKNOWLEDGMENTS

We acknowledge the help of numerous individuals including: Peter Hehanussa, William Napier, Mike Dutton, Matthew Orr, Greg Kane, Paul Kenward, Ezra Kulczycki, Deqie Tetradiono, Lili Lubis, Elisabeth Sabo, Gadis Sri Haryani, Sinyo Rio, CarriAyne Jones, Dullah, and Sarah Bungin. Andrew O'Neill helped with the phylogenetic analyses. Donald Canfield, Alexander Treusch, Daniel Stolper, Brad Tebo, and George Luther are thanked for helpful discussions. Funding was kindly provided by NSERC, INCO Canada Ltd., PT INCO Tbk, KU Geology Associates. S. A. C. was supported by a NSERC IPGS sponsored by INCO Canada Ltd. We also thank the Québec-Ocean Research Center and their staff for calibrating and lending the SeaBird SBE-19 CTD, as well as the GEOTOP Research Center, specifically Dr. Jean-François Hélie, for the ΣCO_2 stable isotopic measurements. We also acknowledge two anonymous reviewers for their comments on an earlier submission of this manuscript as well as the three anonymous reviewers for *Geobiology*. We thank Kurt Konhauser for editorial handling.

REFERENCES

Bastviken D, Cole J, Pace M, Tranvik L (2004) Methane emissions from lakes: dependence of lake characteristics, two regional assessments, and a global estimate. *Global Biogeochemical Cycles* **18**, 1–12.

Bastviken D, Cole JJ, Pace ML, Van de Bogert MC (2008) Fates of methane from different lake habitats: connecting whole-lake budgets and CH_4 emissions. *Journal of Geophysical Research-Biogeochemistry* **113**, 13.

Baur ME, Hayes JM, Studley SA, Walter MR (1985) Millimeter-scale variations of stable isotope abundances in carbonates from banded iron-formations in the Hamersley group of Western-Australia. *Economic Geology* **80**, 270–282.

Beal EJ, House CH, Orphan VJ (2009) Manganese- and iron-dependent marine methane oxidation. *Science* **325**, 184–187.

Becker RH, Clayton RN (1972) Carbon isotopic evidence for origin of a banded iron-formation in Western Australia. *Geochimica et Cosmochimica Acta* **36**, 577–595.

van Bodegom P, Stams F, Mollema L, Boeke S, Leffelaar P (2001) Methane oxidation and the competition for oxygen in the rice rhizosphere. *Applied and Environmental Microbiology* **67**, 3586–3597.

van Bodegom PM, Scholten JCM, Stams AJM (2004) Direct inhibition of methanogenesis by ferric iron. *FEMS Microbiology Ecology* **49**, 261–268.

Boetius A, Ravenschlag K, Schubert CJ, Rickert D, Widdel F, Gieseke A, Amann R, Jorgensen BB, Witte U, Pfannkuche O (2000) A marine microbial consortium apparently mediating anaerobic oxidation of methane. *Nature* **407**, 623–626.

Brauer SL, Cadillo-Quiroz H, Yashiro E, Yavitt JB, Zinder SH (2006a) Isolation of a novel acidiphilic methanogen from an acidic peat bog. *Nature* **442**, 192–194.

Brauer SL, Yashiro E, Ueno NG, Yavitt JB, Zinder SH (2006b) Characterization of acid-tolerant H_2/CO_2-utilizing methanogenic enrichment cultures from an acidic peat bog in New York State. *FEMS Microbiology Ecology* **57**, 206–216.

Cadillo-Quiroz H, Yavitt JB, Zinder SH (2009) *Methanosphaerula palustris* gen. nov., sp nov., a hydrogenotrophic methanogen isolated from a minerotrophic fen peatland. *International Journal of Systematic and Evolutionary Microbiology* **59**, 928–935.

Caldwell SL, Laidler JR, Brewer EA, Eberly JO, Sandborgh SC, Colwell FS (2008) Anaerobic oxidation of methane: mechanisms, bioenergetics, and the ecology of associated microorganisms. *Environmental Science & Technology* **42**, 6791–6799.

Canfield DE, Thamdrup B, Hansen JW (1993) The anaerobic degradation of organic-matter in Danish coastal sediments – iron reduction, manganese reduction, and sulfate reduction. *Geochimica et Cosmochimica Acta* **57**, 3867–3883.

Canfield DE, Kristensen E, Thamdrup B (2005) *Aquatic Geomicrobiology*, Elsevier, San Diego.

Canfield DE, Rosing MT, Bjerrum C (2006) Early anaerobic metabolisms. *Philosophical Transactions of the Royal Society B-Biological Sciences* **361**, 1819–1834.

Capone DG, Kiene RP (1988) Comparison of microbial dynamics in marine and fresh-water sediments – contrasts in anaerobic carbon catabolism. *Limnology and Oceanography* **33**, 725–749.

Crowe SA, Pannalal SJ, Fowle DA, Cioppa MT, Symons DTA, Haffner GD, Fryer BJ, McNeely R, Sundby B, Hehanussa PE (2004) Biogeochemical cycling in Fe-rich sediments from Lake Matano, Indonesia. In *13th International Symposium on Water-Rock Intera* (eds Torres-Alvarado IS, Birkle P), Saratoga Springs. USA, pp. 1185–1189.

Crowe SA, Jones C, Katsev S, Magen C, O'Neill AH, Sturm A, Canfield DE, Haffner GD, Mucci A, Sundby B, Fowle DA (2008a) Photoferrotrophs thrive in an Archean Ocean analogue. *Proceedings of the National Academy of Sciences of the United States of America* **105**, 15938–15943.

Crowe SA, O'Neill AH, Katsev S, Hehanussa P, Haffner GD, Sundby B, Mucci A, Fowle DA (2008b) The biogeochemistry of tropical lakes: a case study from Lake Matano, Indonesia. *Limnology and Oceanography* **53**, 319–331.

Delong EF (1992) Archaea in coastal marine environments. *Proceedings of the National Academy of Sciences of the United States of America* **89**, 5685–5689.

DeSantis TZ, Hugenholtz P, Larsen N, Rojas M, Brodie EL, Keller K, Huber T, Dalevi D, Hu P, Andersen GL (2006) Greengenes, a chimera-checked 16S rRNA gene database and workbench compatible with ARB. *Applied and Environmental Microbiology* **72**, 5069–5072.

Diaz RJ, Rosenberg R (1995) Marine benthic hypoxia: a review of its ecological effects and the behavioural responses of benthic macrofauna. *Oceanography and Marine Biology* **33**, 245–303.

Eller G, Kanel LK, Kruger M (2005) Cooccurrence of aerobic and anaerobic methane oxidation in the water column of Lake Plusssee. *Applied and Environmental Microbiology* **71**, 8925–8928.

Ettwig KF, Shima S, van de Pas-Schoonen KT, Kahnt J, Medema MH, op den Camp HJM, Jetten MSM, Strous M (2008) Denitrifying bacteria anaerobically oxidize methane in the absence of Archaea. *Environmental Microbiology* **10**, 3164–3173.

Fowle DA, Crowe SA, O'Neill AH, Haffner GD, Sundby B, Mucci A (2006) Microbial ecology and the link between sediment respiration and sediment-water exchange in Lake Matano. In *Symposium on the Malili Lakes Limnology and Ecology* (eds Hehanussa PE, Haryani GS, Ridwansyah I). Jakarta, p. 7.

Gal'chenko VF (2004) On the problem of anaerobic methane oxidation. *Microbiology* **73**, 599–608.

Gieskes JM, Rogers WC (1973) Alkalinity determination in interstitial waters of marine sediments. *Journal of Sedimentary Petrology* **43**, 272–277.

Golightly JP (1981) Nickeliferous laterite deposits. *Economic Geology* **75th Aniversary Volume**, 710–735.

Guindon S, Gascuel O (2003) A simple, fast, and accurate algorithm to estimate large phylogenies by maximum likelihood. *Systematic Biology* **52**, 696–704.

Hall PO, Aller RC (1992) Rapid, small-volume, flow-injection analysis for ΣCO_2 and NH_4^+ in marine and fresh-waters. *Limnology and Oceanography* **37**, 1113–1119.

Hayes J (1983) Geochemical evidence bearing on the origin of aerobiosis, a speculative hypothesis. In *Earth's Earliest Biosphere, its Origin and Evolution* (ed. Schopf J). Princeton University Press, Princeton, pp. 291–301.

Hinrichs KU, Hayes JM, Sylva SP, Brewer PG, DeLong EF (1999) Methane-consuming archaebacteria in marine sediments. *Nature* **398**, 802–805.

Huelsenbeck JP, Ronquist F (2001) MRBAYES: Bayesian inference of phylogenetic trees. *Bioinformatics* **17**, 754–755.

Imachi H, Sakai S, Sekiguchi Y, Hanada S, Kamagata Y, Ohashi A, Harada H (2008) *Methanolinea tarda* gen. nov., sp nov., a methane-producing archaeon isolated from a methanogenic digester sludge. *International Journal of Systematic and Evolutionary Microbiology* **58**, 294–301.

Iversen N, Oremland RS, Klug MJ (1987) Big Soda Lake (Nevada) .3. pelagic methanogenesis and anaerobic methane oxidation. *Limnology and Oceanography* **32**, 804–814.

Jimenez-Lopez C, Romanek CS (2004) Precipitation kinetics and carbon isotope partitioning of inorganic siderite at 25 degrees C and 1 atm. *Geochimica et Cosmochimica Acta* **68**, 557–571.

Katsev S, Crowe SA, Mucci A, Sundby B, Nomosatryo S, Haffner GD, Fowle DA (2010) Mixing and its effects on biogeochemistry in the persistently stratified, deep, tropical Lake Matano, Indonesia. *Limnology and Oceanography* **55**, 763–776.

Kessler JD, Reeburgh WS (2005) Preparation of natural methane samples for stable isotope and radiocarbon analysis. *Limnology and Oceanography-Methods* **3**, 408–418.

King GM, Roslev P, Skovgaard H (1990) Distribution and rate of methane oxidation in sediments of the Florida everglades. *Applied and Environmental Microbiology* **56**, 2902–2911.

Knittel K, Boetius A (2009) Anaerobic oxidation of methane: progress with an unknown process. *Annual Review of Microbiology* **63**, 311–334.

Konhauser KO, Newman DK, Kappler A (2005) The potential significance of microbial Fe(III) reduction during deposition of Precambrian banded iron formations. *Geobiology* **3**, 167–177.

Lane D (1991) S/23S rRNA sequencing. In *Nucleic Acid Techniques in Bacterial Systemati* (eds Stackebrandt E, Debroas D, Fonty G). Wiley, New York, pp. 115–175.

van der Lee J (1993) *CHESS, Another Speciation and Surface Complexation Computer Code*. CIG-Ecole des Mines de Paris, Fontainebleau, France.

Lehours AC, Bardot C, Thenot A, Debroas D, Fonty G (2005) Anaerobic microbial communities in Lake Pavin, a unique meromictic lake in France. *Applied and Environmental Microbiology* **71**, 7389–7400.

Lehours AC, Batisson I, Guedon A, Mailhot G, Fonty G (2009) Diversity of culturable bacteria, from the anaerobic zone of the meromictic Lake Pavin, able to perform dissimilatory-iron reduction in different *in vitro* conditions. *Geomicrobiology Journal* **26**, 212–223.

Lewis E, Wallace DWR (1998) *Program Developed for CO_2 System Calculations. ORNL/CDIC-105*. Carbon Dioxide Information Analysis Center, Oak Ridge National Laboratory, U.S. Department of Energy, Oak Ridge, Tennessee.

Lloyd KG, Lapham L, Teske A (2006) Anaerobic methane-oxidizing community of ANME-1b archaea in hypersaline Gulf of Mexico sediments. *Applied and Environmental Microbiology* **72**, 7218–7230.

Luther GW (2005) Manganese(II) oxidation and Mn(IV) reduction in the environment – two one-electron transfer steps versus a single two-electron step. *Geomicrobiology Journal* **22**, 195–203.

Luther GW, Glazer B, Ma SF, Trouwborst R, Shultz BR, Druschel G, Kraiya C (2003) Iron and sulfur chemistry in a stratified lake: evidence for iron-rich sulfide complexes. *Aquatic Geochemistry* **9**, 87–110.

Martens CS, Albert DB, Alperin MJ (1999) Stable isotope tracing of anaerobic methane oxidation in the gassy sediments of Eckernforde Bay, German Baltic Sea. *American Journal of Science* **299**, 589–610.

Megonigal JP, Schlesinger WH (1997) Enhanced CH_4 emissions from a wetland soil exposed to elevated CO_2. *Biogeochemistry* **37**, 77–88.

Millero FJ, Sotolongo S, Izaguirre M (1987) The oxidation-kinetics of Fe(II) in seawater. *Geochimica et Cosmochimica Acta* **51**, 793–801.

Morgan JJ (2005) Kinetics of reaction between O_2 and Mn(II) species in aqueous solutions. *Geochimica et Cosmochimica Acta* **69**, 35–48.

Nauhaus K, Treude T, Boetius A, Kruger M (2005) Environmental regulation of the anaerobic oxidation of methane: a comparison of ANME-I and ANME-II communities. *Environmental Microbiology* **7**, 98–106.

Orphan VJ, House CH, Hinrichs KU, McKeegan KD, DeLong EF (2001) Methane-consuming archaea revealed by directly coupled isotopic and phylogenetic analysis. *Science* **293**, 484–487.

Raghoebarsing AA, Pol A, van de Pas-Schoonen KT, Smolders AJP, Ettwig KF, Rijpstra WIC, Schouten S, Damste JSS, Op den Camp HJM, Jetten MSM, Strous M (2006) A microbial consortium couples anaerobic methane oxidation to denitrification. *Nature* **440**, 918–921.

Reeburgh WS (1996) Soft spots in the global methane budget. In *Microbial Growth on C1 Compounds* (ed. Lidstrom Frt ME). Kluwer Academic, Dordrecht, pp. 334–342.

Reeburgh WS (2007) Oceanic methane biogeochemistry. *Chemical Reviews* **107**, 486–513.

Reeburgh WS, Ward BB, Whalen SC, Sandbeck KA, Kilpatrick KA, Kerkhof LJ (1991) Black Sea methane geochemistry. *Deep-Sea Research* **38**, S1189–S1210.

Roden EE (2003) Fe(III) oxide reactivity toward biological versus chemical reduction. *Environmental Science & Technology* **37**, 1319–1324.

Roden EE, Urrutia MM (1999) Ferrous iron removal promotes microbial reduction of crystalline iron(III) oxides. *Environmental Science & Technology* **33**, 1847–1853.

Roden EE, Urrutia MM (2002) Influence of biogenic Fe(II) on bacterial crystalline Fe(III) oxide reduction. *Geomicrobiology Journal* **19**, 209–251.

Roden EE, Wetzel RG (1996) Organic carbon oxidation and suppression of methane production by microbial Fe(III) oxide reduction in vegetated and unvegetated freshwater wetland sediments. *Limnology and Oceanography* **41**, 1733–1748.
Roden EE, Wetzel RG (2003) Competition between Fe(III)-reducing and methanogenic bacteria for acetate in iron-rich freshwater sediments. *Microbial Ecology* **45**, 252–258.
Schmid M, Halbwachs M, Wehrli B, Wuest A (2005) Weak mixing in Lake Kivu: new insights indicate increasing risk of uncontrolled gas eruption. *Geochemistry Geophysics Geosystems* **6**, Q07009, 11 pp.
Schubert CJ, Coolen MJL, Neretin LN, Schippers A, Abbas B, Durisch-Kaiser E, Wehrli B, Hopmans EC, Damste JSS, Wakeham S, Kuypers MMM (2006) Aerobic and anaerobic methanotrophs in the Black Sea water column. *Environmental Microbiology* **8**, 1844–1856.
Strous M, Jetten MSM (2004) Anaerobic oxidation of methane and ammonium. *Annual Review of Microbiology* **58**, 99–117.
Stuiver M, Polach HA (1977) Reporting of C-14 data – discussion. *Radiocarbon* **19**, 355–363.
Ueno Y, Yamada K, Yoshida N, Maruyama S, Isozaki Y (2006) Evidence from fluid inclusions for microbial methanogenesis in the early Archaean era. *Nature* **440**, 516–519.
Vetriani C, Tran HV, Kerkhof LJ (2003) Fingerprinting microbial assemblages from the oxic/anoxic chemocline of the Black Sea. *Applied and Environmental Microbiology* **69**, 6481–6488.
Whiticar MJ (1999) Carbon and hydrogen isotope systematics of bacterial formation and oxidation of methane. *Chemical Geology* **161**, 291–314.
Wise MG, McArthur JV, Shimkets LJ (1999) Methanotroph diversity in landfill soil: isolation of novel type I and type II methanotrophs whose presence was suggested by culture-independent 16S ribosomal DNA analysis. *Applied and Environmental Microbiology* **65**, 4887–4897.
Yao WS, Byrne RH, Waterbury RD (1998) Determination of nanomolar concentrations of nitrite and nitrate in natural waters using long path length absorbance spectroscopy. *Environmental Science & Technology* **32**, 2646–2649.
Zehnder AJB, Brock TD (1980) Anaerobic methane oxidation – occurrence and ecology. *Applied and Environmental Microbiology* **39**, 194–204.
Zhang YX, Kling GW (2006) Dynamics of lake eruptions and possible ocean eruptions. *Annual Review of Earth and Planetary Sciences* **34**, 293–324.

APPENDIX 1 (MODELING ISOTOPE FLUXES)

We calculate the methane oxidation rate necessary to sustain the negative excursion in $\delta^{13}C_{\Sigma CO2}$ observed at 122 m against the diffusion of isotopically heavier ΣCO_2. This rate can be estimated by solving reaction-diffusion equations for both carbon isotopes. At steady state:

$$\frac{d}{dz}\left(K_z\frac{d[^{13}C_{\Sigma CO_2}]}{dz}\right)+R_{13}+\frac{[^{13}C_{\Sigma CO_2}]}{[^{13}C_{\Sigma CO_2}]+[^{12}C_{\Sigma CO_2}]}\sum R=0$$
$$\frac{d}{dz}\left(K_z\frac{d[^{12}C_{\Sigma CO_2}]}{dz}\right)+R_{12}+\frac{[^{12}C_{\Sigma CO_2}]}{[^{13}C_{\Sigma CO_2}]+[^{12}C_{\Sigma CO_2}]}\sum R=0 \quad (3)$$

where R_{13} and R_{12} are the required rates of oxidation of ^{13}C and ^{12}C methane, respectively. The terms 'R' with various subscripts are the rates of all reactions that produce or consume ΣCO_2 but do not modify its isotopic composition. The ratio of R_{12} and R_{13} can be expressed in terms of the isotopic composition of the reactant methane:

$$R_{12}/R_{13}=\alpha[^{12}C_{CH_4}]/[^{13}C_{CH_4}],$$

where α is an isotope fractionation factor for AOM and is equal to 1.012 (Martens *et al.*, 1999). Expressing the ΣR from equation 3 and substituting it into equation 4, one obtains the rate of reaction:

$$R=R_{12}+R_{13}\approx R_{12}=\frac{\lambda_{\Sigma CO_2}}{\lambda_{\Sigma CO_2}+\lambda_{CH_4}}\times\left\lfloor\frac{1}{\lambda_{\Sigma CO_2}}\frac{d}{dz}\left(K_z\frac{d[^{13}C_{\Sigma CO_2}]}{dz}\right)-\frac{d}{dz}\left(K_z\frac{d[^{12}C_{\Sigma CO_2}]}{dz}\right)\right\rfloor \quad (4)$$

where $\lambda_{\Sigma CO2}$ and λ_{CH_4} are the ratios of ^{13}C to ^{12}C in ΣCO_2 and CH_4, respectively. By calculating the derivatives from discrete measured values, substituting $\gamma_{\Sigma CO2}$ and γ_{CH_4} for their respective $\delta^{13}C$ values, and using a K_z of 0.16 m^2 day^{-1}, we obtain $R = 5\times10^{-7}$ mol L^{-1} day^{-1} (3.5×10^{-10} mol L^{-1} min^{-1}). This is comparable to the volume-specific rates of net CH_4 consumption calculated from the concentration profile (a gradient of 0.018 mol m^{-4}, K_z of 0.16 m^2 day^{-1}) and assuming that CH_4 consumption occurs within a 10 m depth interval.

APPENDIX 2 (COMPETITION BETWEEN METHANOTROPHS AND FE(II) FOR O_2)

The rate of oxygen consumption by Fe(II) can be approximated by a second-order kinetic law (Millero *et al.*, 1987):

$$\frac{\partial[O_2]}{\partial t}=k\,[Fe(II)]\,[O_2] \quad (5)$$

where k is the rate constant (mol^{-1} L min^{-1}). The rate of oxygen consumption by methanotrophs follows Monod kinetics (van Bodegom *et al.*, 2001):

$$\frac{\partial[O_2]}{\partial t}=\frac{\mu_{max}[O_2]B}{(K_{S,O_2}+[O_2])\,\Upsilon} \quad (6)$$

where μ_{max} is the maximum specific growth rate (min^{-1}), $K_{S,O2}$ is the Monod substrate half-saturation constant for O_2 (mol L^{-1}), B is the microbial cell density (moles microbial C L^{-1}), and Υ is the dimensionless apparent yield (the molar ratio of substrate used to biomass produced).

Table 4 Parameters for kinetic calculations

Parameter	Value	Source
μ_{max}	2.0×10^{-3} min^{-1}	van Bodegom *et al.* (2001)
K_{SO2}	6.7×10^{-6} mol L^{-1}	van Bodegom *et al.* (2001)
Y_m	0.296	van Bodegom *et al.* (2001)
K	102.19 mol^{-1} kg min^{-1}	Millero *et al.* (1987)
[Fe(II)]	3.5×10^{-6} to 1.0×10^{-4} mol L^{-1}	
$[O_2]$	10^{-9} to 10^{-4}mol L^{-1}	
Cell density	10^{-4} to 10^{-6} cells mL^{-1}	
C content of methanotroph cell	6.23×10^{-14} mol C $cell^{-1}$	van Bodegom *et al.*, (2001)

For typical parameter values (Table 4), competition for oxygen between aerobic methanotrophy and Fe(II) oxidation is illustrated graphically in Fig. 9A. Irrespective of cell density, methanotrophic oxygen consumption plateaus when the oxygen concentration exceeds 1 μmol L^{-1}, whereas abiotic O_2 consumption by Fe(II) is log-linear at all O_2 concentrations. The percentage of O_2 consumption by methanotrophs vs. total O_2 consumption by methanotrophy and Fe(II) oxidation as a function of ambient O_2 concentration is shown in Fig. 9B for a range of Fe(II) concentrations and a cell density of 10^5 cells mL^{-1}. At low O_2 concentrations, a higher percentage of oxygen is consumed by methanotrophs than by abiotic Fe(II) oxidation. At methanotroph cell densities of 10^5 cells mL^{-1}, typical of microaerophilic zones in methane-rich chemoclines (Eller *et al.*, 2005; Lehours *et al.*, 2005), and Fe concentrations of 35 μmol L^{-1}, methanotrophy consumes approximately 50% of the available O_2 at O_2 concentrations less than 1 μmol L^{-1}.

Using the Monod expression for aerobic methanotrophy (equation 6), cell densities up to 10^5 cells mL^{-1}, and oxygen concentrations up to 5 nmol L^{-1} (the O_2 concentration at 120 m depth was estimated at 4.7 nmol L^{-1} by fitting a logarithmic function (R^2 = 0.92) to the O_2 concentration profile between 105 and 110 m and extrapolating to 120 m depth), we estimate that the rate of aerobic methane oxidation is at most 3.1×10^{-11} mol L^{-1} min^{-1}. Note that using the measured Fe(II) concentrations and the solubility limit of Fe(III) at pH 7.21 gives an estimated pe of 5.58 which, at equilibrium, translates to O_2 concentrations of 1.4×10^{-26} nmol L^{-1}. Hence, unless O_2 is rapidly supplied to 120 m depth, it is likely present at concentrations much lower than the rough estimates gleaned from the O_2 concentration profile.

APPENDIX 3 (ENERGY YIELDS)

Table 5 Free energy yield (kJ mol^{-1}) for reaction 5 assuming that concentrations are equal to activities (i.e., ideal solution) and a pH of 7.0

	HCO_3^- 10^{-3} M				HCO_3^- 10^{-2} M			
$CH_{4(aq)}$ (M)	Fe^{2+}(10^{-6} M)	Fe^{2+}(10^{-5} M)	Fe^{2+}(10^{-4} M)	Fe^{2+}(10^{-3} M)	Fe^{2+}(10^{-6} M)	Fe^{2+}(10^{-5} M)	Fe^{2+}(10^{-4} M)	Fe^{2+}
10^{-6}	−229.9	−184.2	−138.6	−92.9	−224.2	−178.5	−132.9	−87.2
10^{-5}	−235.6	−189.9	−144.3	−98.6	−229.9	−184.2	−138.6	−92.9
10^{-4}	−241.3	−195.6	−150.0	−104.4	−235.6	−189.9	−144.3	−98.6
10^{-3}	−247.0	−201.3	−155.7	−110.1	−241.3	−195.6	−150.0	−104.4

Table 6 Free energy yield (kJ mol^{-1}) for reaction 6 assuming that concentrations are equal to activities (i.e., ideal solution) and a pH of 7.0

	HCO_3^- 10^{-3} M				HCO_3^- 10^{-2} M			
$CH_{4(aq)}$ (M)	Mn^{2+}(10^{-6} M)	Mn^{2+}(10^{-5} M)	Mn^{2+}(10^{-4} M)	Mn^{2+}(10^{-3} M)	Mn^{2+}(10^{-6} M)	Mn^{2+}(10^{-5} M)	Mn^{2+}(10^{-4} M)	Mn^{2+}(10^{-3} M)
10^{-6}	−630.2	−607.4	−584.5	−561.7	−624.5	−601.7	−578.8	−556.0
10^{-5}	−635.9	−613.1	−590.2	−567.4	−630.2	−607.4	−584.5	−561.7
10^{-4}	−641.6	−618.8	−595.9	−573.1	−635.9	−613.1	−590.2	−567.4
10^{-3}	−647.3	−624.5	−601.7	−578.8	−641.6	−618.8	−595.9	−573.1

APPENDIX 4 (BACTERIAL PHYLOGENY)

Figure 11 shows the phylogeny of non-chimeric clones sequenced from PCR products generated using primers to target known aerobic methanotrophs. These clones cluster within the β subdivision of the proteobacteria, whereas members of Type I and Type II methanotrophs all belong to the γ and α subdivisions, respectively.

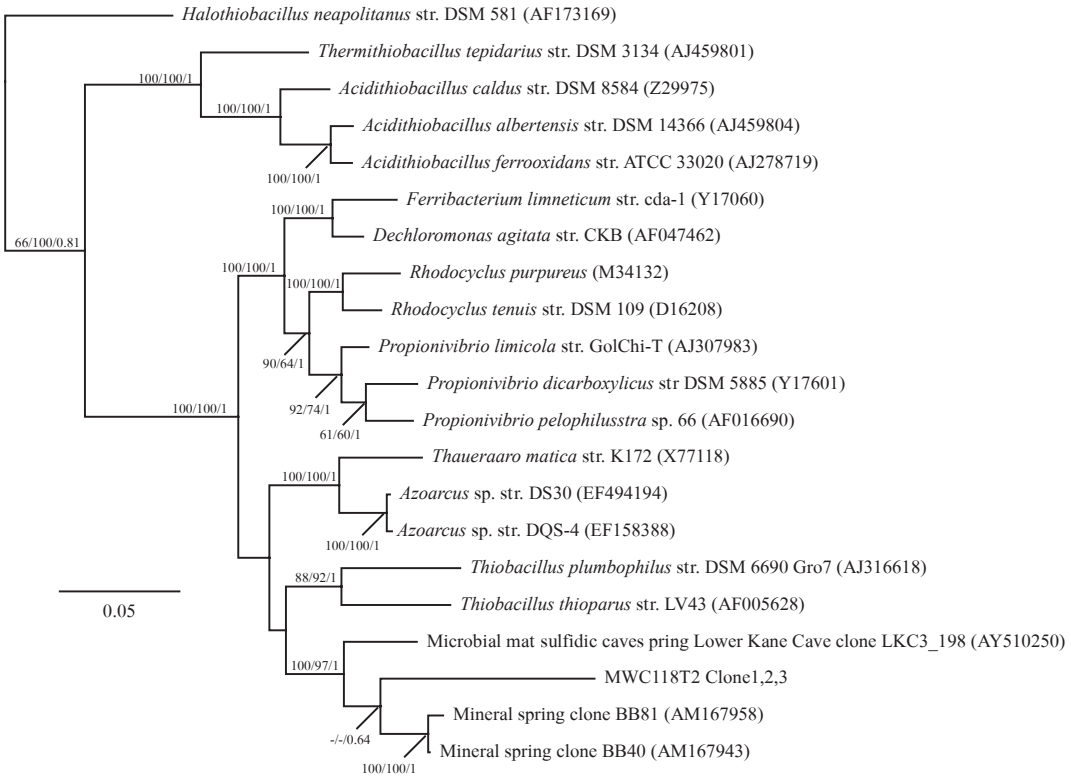

Fig. 11 Phylogenetic tree displaying the affiliations of 16S rRNA gene sequences obtained from 118 m depth in Lake Matano using PCR primers designed to target aerobic methanotrophs (MWC118T2). The tree includes reference species in addition to the nearest non-chimeric neighbors identified using the Greengenes Simrank tool. The tree was constructed using the PHYML maximum likelihood algorithm. The numbers at the branching nodes represent bootstrap support for neighbor joining (1000 bootstrap replications) and maximum likelihood (100 bootstrap replications) in addition to probability from Bayesian inference (NJ/ML/BI). Bootstrap support of less than 60% and probabilities of less than 0.6 are not shown. *Escherichia coli* K12 (M87049) was used as an outgroup to root the tree.